



## Regular Article

## Effect of sphingosine on domain morphology in giant vesicles

Raina Georgieva<sup>a</sup>, Kamen Koumanov<sup>a</sup>, Albena Momchilova<sup>a</sup>, Cedric Tessier<sup>b</sup>, Galya Staneva<sup>a,\*</sup><sup>a</sup> Institute of Biophysics, Bulgarian Academy of Sciences, Acad. G. Bonchev Str., Bl. 21, 1113 Sofia, Bulgaria<sup>b</sup> Université Pierre et Marie Curie-Paris 6, UMRS 7203CNRS-ENS, CHU St. Antoine, 27 rue Chaligny, 75012 Paris, France

## ARTICLE INFO

## Article history:

Received 5 May 2010

Accepted 10 July 2010

Available online 15 July 2010

## Keywords:

Sphingosine

Cholesterol

Sphingomyelin

Membrane domains

Rafts

Lipid signaling pathway

Apoptosis

## ABSTRACT

Sphingosine is a bioactive molecule which is known to participate in the regulation of a number of cellular processes such as apoptosis, cell differentiation, growth, etc. Sphingosine was observed to exhibit different domain morphology depending on the surrounding lipid matrix in biomimetic systems such as giant vesicles. Our current results showed that in a glycerophospholipid matrix sphingosine segregated in gel leaf-like domains whereas cholesterol presence increased its miscibility by melting gel domains in a concentration-dependent manner. Sphingosine and cholesterol did not form merging liquid domains on the micron scale as observed for sphingomyelin and cholesterol. However, we were able to visualize that sphingosine appears as a stabilizer and amplifier of domains in liquid-ordered phase by increasing the temperature of their formation and fraction. These results imply that sphingosine acts as a modulator of the lipid domain formation and thus it could exert its biological role, not only through direct binding to proteins, but also indirectly by influencing their sorting in membranes and modulating the processes of signal transduction.

© 2010 Elsevier Inc. All rights reserved.

## 1. Introduction

Interest in sphingolipids and their metabolites has grown very rapidly since the establishment of their important role in cell signaling. The mechanisms of action of ceramide and sphingosine-1-phosphate have been particularly well studied. It is known that these two sphingolipids exhibit opposite effects on various cellular processes such as apoptosis, cell differentiation, growth, etc. Sphingosine-1-phosphate exerts an inhibitory effect on apoptosis unlike ceramide which stimulates this process [1–3]. The interest of many authors has been attracted by the so-called “ceramide/sphingosine-1-phosphate rheostat”, i.e. the ratio between these two lipids could determine the fate of a cell – apoptosis in case of high ceramide levels or cell survival if sphingosine-1-phosphate predominates [4]. However, the intermediate product in the metabolic chain “ceramide/sphingosine-1-phosphate”, sphingosine, has received less attention. Studies related to its mechanism of action are quite incomplete, although its essential role in the functioning of the “ceramide/sphingosine-1-phosphate rheostat” is more than obvious. It is assumed that cellular sphingosine (SPH) is formed exclusively as a result of ceramide degradation whereas its eventual de novo synthesis does not occur [5].

Sphingosine generated by neutral ceramidase could also be found in the plasma membrane outer monolayer. This indicates that neutral ceramidase can actively participate in ceramide metabolism at plasma membrane level and thus be a mediator in

the production of sphingosine-1-phosphate [6]. According to some authors the presence of acid sphingomyelinase and neutral ceramidase at the cellular surface suggests that membrane rafts are the site for generation of sphingosine [7,8]. Hengst et al. [9] demonstrate that endogenous human sphingosine kinase 1 and its substrate, D-erythro-sphingosine, reside in the plasma membrane lipid raft domains. These facts support the key role of SPH in the sphingomyelin signaling pathway and the importance of plasma membrane lipid microdomains in the performance of these processes.

There is still no data revealing the tendency of SPH molecules to self-aggregate and form microdomains, and to interact with cholesterol, as it is typical for sphingomyelin and the most relevant question in the current study is whether SPH has the ability to form or modulate micron-scale domains in liquid-ordered phase which are considered as a simplified lipid model of rafts at the cellular level.

What we know for the physico-chemical properties of sphingosine is its pKa = 8.9 in membranes which determines the positive charge of this molecule under physiological conditions [10]. Recently Sasaki et al. [11] have shown that the changes in the aggregation structure of sphingosine between pH 6.7 and 9.9 is a shift in the predominant hydrogen-bonding network from intramolecular to intermolecular. The authors presumed that this shift plays a key role in the formation of large sphingosine aggregates which may be important for understanding of certain lysosomal glycosphingolipid storage disorders. Biophysical studies on the phase behavior of mixtures involving sphingosine with dipalmitoyl phosphatidylcholine (DPPC) and dielaidoyl phosphatidylethanolamine (DEPE) [12,13] or phosphatidylserine (PS) and cholesterol [13,14] showed that

\* Corresponding author. Fax: +359 2 9712493.

E-mail address: gstaneva@obzor.bio21.bas.bg (G. Staneva).

SPH rigidified membranes. According to Garmy et al. [15], SPH formed pair-wise condensed complexes with cholesterol. These authors suggested that SPH interacts specifically with cholesterol and inhibits the intestinal Niemann–Pick C1 like 1-dependant transport of micellar cholesterol. Also the pro-apoptotic action of certain receptor systems and various environmental stress factors (such as ionizing radiation, heat shock, oxidative stress) is associated with the signaling cascades launched by CER or SPH. It is assumed that the pre-initiation of apoptosis is lying at the basis of neurodegenerative diseases (for example Alzheimer's disease and Huntington's disease) [16]. It is known that the accumulation of SPH in lysosomes, known as Niemann–Pick (C1) disease, is the initiating factor that alters  $Ca^{2+}$  homeostasis, which in turn leads to accumulation of other sphingolipids and cholesterol [17]. To emphasize the vast physiological role of SPH it should be mentioned that sphingoid bases have been reported to stimulate DNA synthesis [18].

The ability to increase membrane rigidity appears to be a primary property of sphingosine [19]. Probably therein lays the indirect inhibitory effect of SPH on different protein kinase C isoforms [20] as well as its stimulating effect on the activity of DAG kinase and phospholipase C [21,22]. It is well known that these enzymes do not contain a sphingosine-binding site, which excludes the direct influence of SPH on their activity.

It is very likely that the mentioned physiological effects of SPH are due to its impact on the physical state of cell membranes and thus on various functionally active proteins–enzymes, receptors, etc. That is why our current study is devoted to the effect of SPH on the domain morphology in various lipid matrix. Giant unilamellar vesicles (GUVs) comprised of different ratios of natural-occurring lipids such as egg-yolk phosphatidylcholine (PC), egg-yolk sphingomyelin (SM), bovine brain sphingosine (SPH) and cholesterol (CHOL). Different patterns of domain formation in the micron scale were visualized using fluorescence microscopy in PC/SPH binary mixtures, PC/SPH/CHOL; PC/SM/CHOL ternary and PC/SPH/SM/CHOL quaternary mixtures. We were able to determine the temperature of micron-scale domain formation, identification of domain shape and size as well as their dynamics like for example their capacity to merge. The binary mixtures allowed us to visualize the formation of gel leaf-like domains composed of self-aggregated SPH molecules in glycerophospholipid matrix. The next step was to establish the effect of CHOL in a lipid bilayer containing SPH (ternary mixtures) in order to be able to answer the question whether SPH and CHOL interact in a manner similar to SM and CHOL as could be presumed in view of the structural analogy between SPH and SM molecules: a common sphingoid base. We observed that SPH and CHOL (PC/SPH/CHOL) did not form liquid domains in micron scale unlike SM and CHOL (round shape and merging domains). In quaternary mixtures we examined the direct SPH influence on the formation of “rafts” type domains and we observed that SPH increases the temperature of domain formation and their fraction. Thus, SPH appears as stabilizer and amplifier of the domains in the liquid-ordered phase.

With this study, we aimed to clarify how SPH, a product of sphingolipid-metabolizing enzymes, affects the lateral organization of lipids in membranes in order to understand how this molecule works not only on intra-cellular organelles (sphingolipid-enriched lysosomes) but also in the extra-cellular space, including the outer monolayer of plasma membranes.

## 2. Materials and methods

### 2.1. Commercial reagents

Egg-yolk  $\alpha$ -phosphatidylcholine, egg-yolk sphingomyelin, bovine brain sphingosine and the fluorescent lipid analogue

$\alpha$ -phosphatidylethanolamine-N-(lissamine rhodamine B sulfonyl)-Rhod-PE (Chicken) were obtained from Avanti Polar Lipids, Alabaster, AL and used without further purification. The distribution of fatty acids in egg phosphatidylcholine consisted of 34% C16:0, 2% C16:1, 11% C18:0, 32% C18:1, 18% C18:2 and 3% C20:4 and for egg sphingomyelin it was 84% C16:0, 6% C18:0, 2% C20:0, 4% C22:0 and 4% C24:0. Cholesterol was from Sigma–Aldrich, St. Quentin-Fallavier, France. The buffer Hepes was also purchased from Sigma–Aldrich.

### 2.2. Preparation of Giant Unilamellar Vesicles

The electroformation method, developed by Angelova and Dimitrov [23], was used to prepare giant unilamellar vesicles (GUVs). The vesicles were formed in a temperature – controlled chamber in 0.5 mM Hepes buffer, pH 7.4. The temperature was controlled with a Peltier microscope stage at rate of 0.2 °C/min. The vesicles were always formed at 45 °C at which a high yield of vesicles was consistently obtained. Recently, formation of lipid peroxides caused by electrochemical reactions was reported during the vesicle preparation by using ITO-glass electrodes [24,25] unlike GUVs formed by titanium electrodes [24]. Platinum (Pt) electrodes, used under our experimental conditions as well, were not studied in detail and the authors assumed that “it would lead to generation of peroxides because the platinum is not a “valve metal” as it is for the titanium. Ayuyan and Cohen [24] state that only those vesicles that came within proximity of the ITO-glass electrodes could have their lipids electrochemically peroxidized. We did not observe differences in the phase separation between the vesicles attached on the Pt electrodes and those which were far enough. We ascribed this fact not only to the use of Pt electrodes but also to the application of low 300–400 mV peak to peak sine wave voltages and not 1.4 V like in Ayuyan and Cohen's report [24] and even more (up to 10 V) in Zhou et al. [25]. This, of course, makes two to three times longer the time of vesicle preparation. To avoid photo-induced oxidation during the fluorescence observation the following preventive measures were undertaken. Low power illumination, 50 W Hg arc lamp light, and low dye concentration were used (up to 0.8 mol% for epifluorescence measurements) [26]. Also, we accepted as experimental results the phase separation visualized immediately after opening of illumination with exposure time from 300 to 800 ms and not those taken after longer exposure and/or observation time (in the order of minutes). Our results were averaged from at least 10 random vesicles at each temperature of observation and at least three experiments of each lipid mixture. The vesicles were observed using a Zeiss Axiovert 135 microscope equipped with 63× long working distance objective lens (LD Achromplan Ph2). Observations were recorded using Zeiss AxioCam HSm CCD camera connected to an image recording and processing system (Axiovision, Zeiss). The phase morphology of the heterogeneous GUV membranes were followed in phase contrast and in fluorescence by Zeiss filter set 15 ( $E_x/E_m = 546/590$  nm). The headgroup labeled lipid analogue egg Rhod-PE is excluded from the more ordered phase and partitions predominantly in the disordered one. That makes the more ordered phase appear as a dark spot within the bright vesicle membrane. Since there is evidence in the literature that certain lipid markers such as Rhodamine-DPPE and DiIC<sub>18</sub> partition into different phases (gel or liquid-disordered) depending on the local chemical environment [27,28], we checked the studied phase separation by using the followed fluorescent probes: headgroup labeled fluorescent lipid analogue (Texas-red – DPPE) and fatty acid labeled ones (18:1-12:0 NBD-PC and NBD-SPH) (data not shown). Irrespective of the type of the fluorescent probe, none of them showed a reversal of the contrast making bright gel phase (bright leaf-like domains) or making bright liquid-ordered phase (bright round shape domains) on dark

liquid background in all of the studied lipid mixtures. Difference in the temperature of domain formation and their shape was not observed as well. Therefore, it can be concluded that all fluorescent probes, used in this study, were partitioned in liquid-disordered phase. The assignment of phases is not problematic in the case of gel/liquid-disordered phase coexistence because gel domains exhibit leaf-like shapes and they are not merging domains. However, when liquid/liquid immiscibility is observed in the membrane bilayer the fluorescent probe assignment of phases would be confused because two phases share similar physico-chemical properties. Higher affinity for disordered phase than for a more compact one is expected for the used by us fluorescent probe-egg-Rhod-PE due to its unsaturated fatty acids which prevent the tight packing of N-acyl chains unlike Rhodamine-DPPE. The same reason is adopted also for all NBD-chain labeled lipid species [29]. Another indirect argument for unambiguous assignment of the dark domains as domains in liquid-ordered phase is related to systematic variations in SM and CHOL concentrations in the mixtures. At low SM and CHOL concentrations the fraction of liquid-ordered domains must be smaller than liquid-disordered.

Micron-scale miscibility transition temperatures were recorded as the temperature at which visible domains appeared and then disappeared as temperature was decreased and then increased (Table 1). This is described in detail by Veatch and Keller [30]. Transition temperature is defined as the average of these two points. Standard deviations correspond to the averaged data from at least 10 vesicles. Integers were taken because experimental errors in transition temperatures had a systematic contribution of  $\pm 1$  °C from the response time of the thermistor. It should be noted that measured transition temperatures correspond to 63x objective magnification.

### 3. Results

#### 3.1. GUVs prepared from phosphatidylcholine/sphingosine (PC/SPH 90/10, 80/20 and 60/40) binary mixtures

To better understand the phase behavior of SPH in complex quaternary mixtures, modeling more closely natural membranes, we started our studies by exploring its phase behavior (in term of domain formation) in three simplified binary mixtures: PC/SPH 90/10, 80/20 and 60/40. The micron-scale miscibility transition temperatures for all studied lipid mixtures are summarized in Table 1.

**Table 1**  
Micron-scale miscibility transition temperature for different series of lipid mixtures.

| Lipid mixture              | $T_{\text{micron-scale miscibility transition temperature}}$                                 |
|----------------------------|----------------------------------------------------------------------------------------------|
| <i>Binary mixtures</i>     |                                                                                              |
| (PC/SPH)                   | $L_{\beta}/L_d$                                                                              |
| 90/10                      | $(10 \pm 2)^{\circ}\text{C}$                                                                 |
| 80/20                      | $(14 \pm 3)^{\circ}\text{C}$                                                                 |
| 60/40                      | $(18 \pm 4)^{\circ}\text{C}$                                                                 |
| <i>Ternary mixtures</i>    |                                                                                              |
| (PC/SPH/CHOL)              | $L_{\beta}/L_d$                                                                              |
| 70/20/10                   | $(14 \pm 3)^{\circ}\text{C}$                                                                 |
| 60/20/20                   | $(10 \pm 3)^{\circ}\text{C}$                                                                 |
| 50/20/30                   | $(6 \pm 2)^{\circ}\text{C}$                                                                  |
| <i>Control mixtures</i>    |                                                                                              |
| (PC/SM/CHOL)               | $L_o/L_d$                                                                                    |
| 50/30/20                   | $(24 \pm 5)^{\circ}\text{C}$                                                                 |
| 30/50/20                   | $(37 \pm 3)^{\circ}\text{C}$                                                                 |
| <i>Quaternary mixtures</i> |                                                                                              |
| (PC/SPH/SM/CHOL)           |                                                                                              |
| 50/20/10/20                | $(18 \pm 3)^{\circ}\text{C}$ ( $L_{\beta}/L_d$ ); $(10 \pm 4)^{\circ}\text{C}$ ( $L_o/L_d$ ) |
| 40/20/20/20                | $(26 \pm 4)^{\circ}\text{C}$ ( $L_o/L_d$ )                                                   |
| 30/20/30/20                | $(37 \pm 2)^{\circ}\text{C}$ ( $L_o/L_d$ )                                                   |

To visualize lipid phase separation, single GUVs composed of 80/20 PC/SPH (Fig. 1) were observed in the wide temperature range from 37 °C to 4 °C. Upon cooling, from 37 °C to 15 °C the vesicles exhibited a homogeneous appearance (Fig. 1a) whereas below 15 °C (Table 1) the formation of dark domains was observed as illustrated by the fluorescence images (Fig. 1b). It should be noted that the resolution upon our experimental conditions was in the order of several micrometers, i.e. the presence of phase separation on the submicron scale (nanometer scale) would not be precluded. The formation of the dark fraction is a consequence of the exclusion of the fluorescent marker egg Rhod-PE from the more ordered phase, represented as dark domains and its partition into the remaining liquid-disordered phase ( $L_d$ ), appearing as a bright phase. Well resolved leaf-like domains were detected at about 10 °C (Fig. 1c) which moved laterally within the plane of the bright lipid phase. The number of petals in the leaf-like domains was usually five, six or eight. Upon further temperature decrease, the leaf-like domains increased their size rather than their number at the given temperature rate (0.5 °C/min). There was often a single leaf-like domain in a vesicle. This temperature effect was probably due to the gradual inclusion of SPH molecules in the dark phase. Furthermore, at low temperatures, the shape of the dark domains became more distinct (Fig. 1e). The leaf-like shape of the domains is determined by the balance between two forces that act on the edge of a domain. The first one is the line tension, which tends to form round shaped domains and the other force is due to the electrostatic repulsions between SPH molecules. The electrostatic repulsive forces are likely to maximize the distance between the molecules within a domain and thus favor the irregular or fractal-like shape of the domains [31,32]. Therefore, the shape of the leaf-like domains is rather governed by long-range electrostatic repulsion rather than by the line tension, which would also explain why fusion between leaf-like domains was never observed in our experiments. The domains tended to attach and form clusters of two (Fig. 1d) or more domains (Fig. 1f). The leaf-like shape of the dark domains and their property to increase gradually in size with temperature reduction, without fusion between them, are typical for domains in gel phase ( $L_{\beta}$ ). They should be composed mainly of SPH since the melting temperature of this lipid has been reported to be about 30–40 °C depending on the pH of the surrounding medium [14,33].

The PC/SPH 90/10 binary mixture is not shown because phase separation occurred at lower temperature (10 °C, Table 1). Even at 4 °C due to the small sizes of the domains it was difficult to identify their shape.

When raising the amount of SPH up to 40 mol% (data not shown) leaf-like domains formed at a higher temperature (18 °C, Table 1). Their number did not vary, but a significant increase in their size was observed compared with the EPC/SPH 80/20 mixture. The number of petals did not vary as well, but the petals became longer.

#### 3.2. GUVs prepared from phosphatidylcholine/sphingosine/cholesterol (PC/SPH/CHOL) ternary mixtures. Effect of cholesterol on SPH domain formation

The domain morphology of three PC/SPH/CHOL ternary mixtures was studied. We examined the effect of CHOL by varying its molar ratio from 10, 20 and 30 mol%. The proportion of SPH was fixed to 20 mol%.

The addition of 10 mol% CHOL to the binary mixture did not change the temperature of domain formation (14 °C, Table 1) as illustrated in Fig. 2a and b. Apparently, there was no significant change in the fraction of the gel domains (Fig. 2b–d). Linear clusters of gel domains were observed at low temperatures (4 °C) (Fig. 2d) just like PC/SPH 80/20 binary mixture (Fig. 1f).

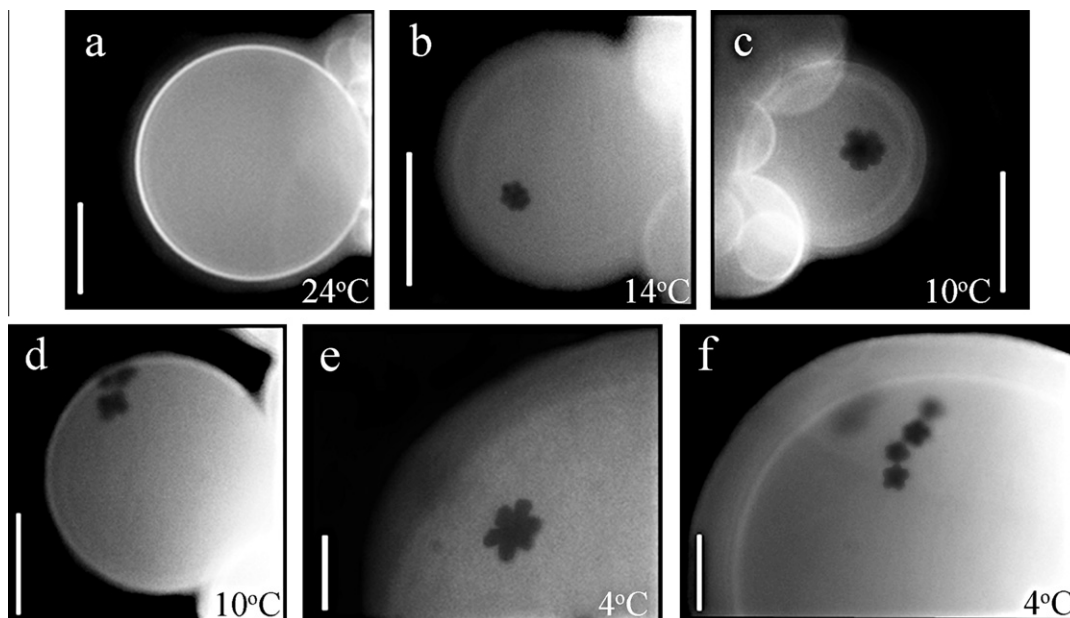


**Fig. 1.** Visualization of  $L_{\beta}/L_d$  phase separation in sphingosine-containing GUVs on the micron scale. PC/SPH 80/20 binary mixture yielded homogeneous vesicles in the temperature range from 37 °C to 15 °C (a). Domain formation at 14 °C (b). Well resolved dark leaf-like domains at 10 °C (c). Clustering of small leaf-like domains at 10 °C (d). Formation of well resolved petals at 4 °C (e). Assembly of two (d) and four (f) domains into clusters at 4 °C. Bar 20  $\mu\text{m}$ .

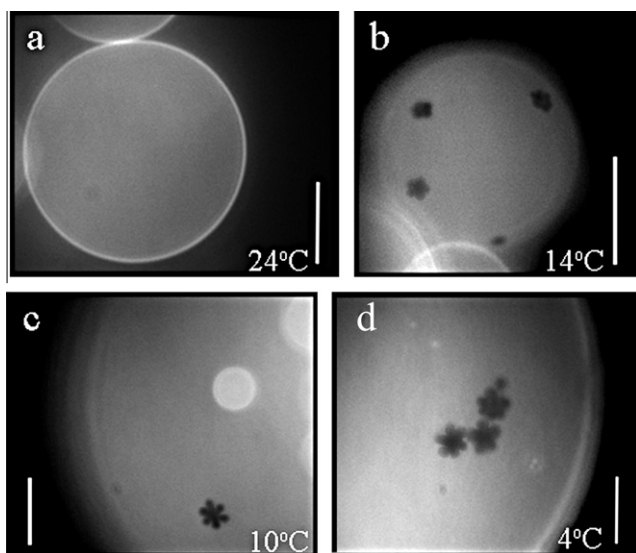


**Fig. 2.**  $L_{\beta}/L_d$  phase separation in a ternary PC/SPH/CHOL 70/20/10 mixture. Homogeneous vesicles in the temperature range from 37 °C to 15 °C (a). Formation of dark leaf-like domains at 14 °C (b) similar to PC/SPH 80/20 binary mixture. Domain growth in size upon cooling (c). Formation of domain clusters at low temperature (d). Bar 20  $\mu\text{m}$ .

Increasing the amount of CHOL to 20 mol% led to a decrease in the temperature of domain formation with about 4 °C compared to 10 mol% (Table 1). Domains formed at 10 °C (Fig. 3a and b). Their size was visibly reduced and that is why their structure remained unresolved. In contrast to this tendency their number was augmenting (Fig. 3b). Despite their large number and nearly round shape, the domains did not increase their size by fusion. Although the domains were enough large, their petals were almost invisible even at 4 °C (Fig. 3c). The fraction of the dark domains was significantly reduced in PC/SPH/CHOL 60/20/20 compared to the control PC/SPH 80/20 mixture (Fig. 1) and the previous PC/SPH/CHOL 70/20/10 (Fig. 2).

At 30 mol% CHOL the formation of the domains was shifted down to 6 °C (Table 1). The common trend in ternary mixtures was that each 10% CHOL led to a decrease in the temperature of domain formation by about 4 °C (Table 1). 30 mol% CHOL further increased the number of SPH gel domains at the expense of their size (data not shown). However, there were a large number of domains in which the number of the petals was reduced to 2–3. It is possible that these are individual domains, attached to each other. If so, their size was too small to allow the visualization of their structure. Overall, the dark domains had a rounded shape, but again they did not fuse with each other. Despite their round shape, they exhibited the properties of solid, gel domains. Raising the amount of cholesterol (to 20 and 30 mol%) exerted also a destabilizing effect on vesicle membranes. Some of the vesicles were shrinking upon cooling (temperature rate 0.5 °C/min) which was not observed for the previous mixtures. This effect was probably due to the high percentage of molecules with one hydrophobic tail in the plane of the membrane bilayer (CHOL + SPH, a total of 40 or 50 mol%) which complicated the study on phase morphology. The statistic in our results was achieved by a greater number of repetitions of the vesicle formation (experiments) than the large number of vesicles in a single experiment.

### 3.3. GUVs prepared from phosphatidylcholine/sphingosine/sphingomyelin/cholesterol (PC/SPH/SM/CHOL) quaternary mixtures. The effects of SM on SPH phase behavior

In this series of experiments the effect of SM on SPH gel domain formation was examined on one hand. On the other, we checked whether the SM–CHOL interactions responsible for the formation of liquid-ordered phase were influenced by SPH presence. For this purpose, the ratio SPH/CHOL was fixed at 20/20, while the proportions of SM varied (10, 20 and 30 mol%).

#### 3.3.1. PC/SPH/SM/CHOL 50/20/10/20

The addition of 10 mol% SM to the ternary PC/SPH/CHOL 60/20/20 mixture (Fig. 3) increased significantly the temperature of domain formation by about 8 °C (Fig. 4a and b), i.e. they were formed

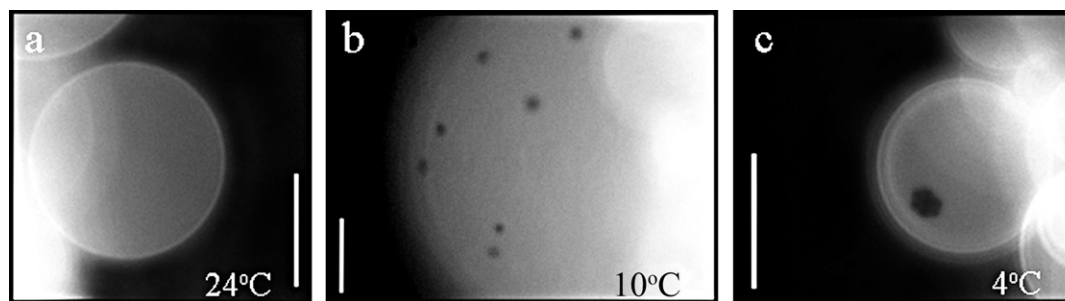


**Fig. 3.**  $L_{\beta}/L_d$  phase separation in a PC/SPH/CHOL 60/20/20 ternary mixture. Homogeneous vesicles in the temperature range from 37 °C to 11 °C (a). Domain formation at 10 °C (b). Domains were characterized with short petals (c). Bar 20  $\mu\text{m}$ .

at 18 °C (Table 1). These dark domains did not fuse but formed clusters (Fig. 4c). Therefore, these domains could be assigned as gel phase, although their petals were hardly visible (Fig. 4b). At about 10 °C dark domains of another type with a different phase behavior appeared (Fig. 4d). They were round shaped and increased in size through fusion (Fig. 4e–g). Such phase behavior is typical for two immiscible liquid phases, liquid-ordered phase ( $L_o$ ) corresponding to the round dark domains and liquid-disordered phase ( $L_d$ ) – assigned to the bright phase of the vesicles. The round shape of the liquid domains is governed by the line tension [29,34]. The line tension acting on the edge of the domain obtains maximum values when two liquid phases coexist due to the loss of energy associated with the creation of phase boundary [29,35]. For example such loss of energy results from the maintaining of about 4 Å hydrophobic mismatch between two liquid phases

due to the difference in thickness of two bilayers in  $L_o$  and  $L_d$  phase state [36,37]. Domains with a shape different from circular or leaf-like were observed at lower temperatures, marked by arrows in Fig. 4e–g. Such an irregular shape, but closer to a circular one, could be a consequence of decreased line tension on the edge of these domains due to the presence of SPH enriched gel phase within the domain or charge dependent effect on the line tension. Thus, we can say figuratively that liquid  $L_o$  domains lose elasticity at the expense of the gain of plasticity.

### 3.3.2. PC/SPH/SM/CHOL 40/20/20/20 and 30/20/30/20

20 mol% SM increased the temperature of  $L_o/L_d$  phase separation to 26 °C (Table 1, Fig. 5a). The equimolar ratio SPH/SM/CHOL exhibited domains with perfectly round shape that quickly grew in size by fusion. As mentioned above such mechanism of growth

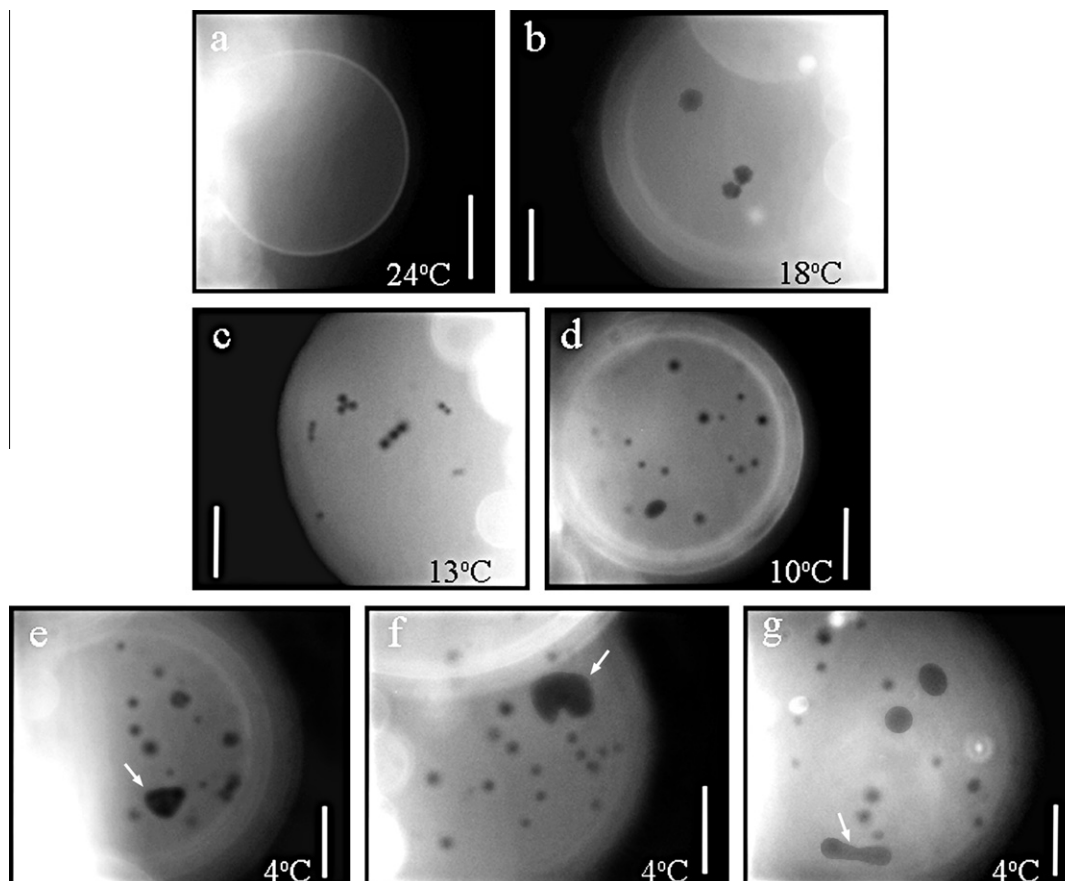


**Fig. 4.** Visualization of phase separation in a PC/SPH/SM/CHOL 50/20/10/20 quaternary mixture. Vesicles exhibited a homogenous appearance from 37 °C to 19 °C (a). Formation of  $L_{\beta}$  domains at 18 °C (b). Clusters of two or three  $L_{\beta}$  domains (c). Formation of  $L_o$  domains at 10 °C (d) and their increase in size by fusion (e–g). Bar 20  $\mu\text{m}$ .

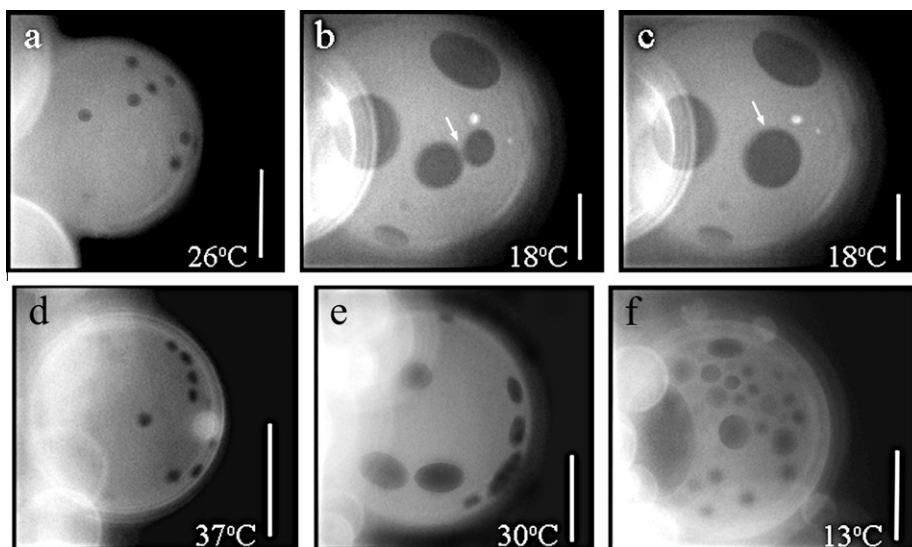


**Fig. 5.**  $L_o/L_d$  phase separation in a PC/SPH/SM/CHOL 40/20/20/20 quaternary mixture (a–c). Formation of  $L_o$  domains at 26 °C (a). Domains before (b) and after fusion (c).  $L_o/L_d$  phase separation in PC/SPH/SM/CHOL 30/20/30/20 (d–f). Formation of  $L_o$  domains at physiological temperature (d). Increasing domain number and size with decreasing temperature (e and f). Bar 20  $\mu\text{m}$ .

can be attributed only to domains existing in  $L_o$  phase (Fig. 5b and c). Domains of leaf-like shape (in gel phase) were not detected. This does not necessarily mean that no gel domains existed in the membrane bilayer. There are at least two possible reasons for the above observation. The first possibility is that phase separation, affected by the presence of SM, consists of domains of a nanometer scale dimension. The second possibility is that the domains are formed within the dark  $L_o$  domains, where the fluorescent marker does not provide enough contrast to visualize them. Even if gel phase is likely to exist in the dark  $L_o$  domains, it is evident that the properties of the  $L_o$  phase are preponderant, leading to fast domains fusion and rapid recovering of the round shape (Fig. 5b and c (marked by arrows)). Upon further increasing of the SM amount in the quaternary mixture, the  $L_o/L_d$  demixing temperature increased (37 °C, Table 1) and  $L_o$  domains were observed at physiological temperature (Fig. 5d). A tendency was observed that the addition of each 10 mol% SM in the series of quaternary mixtures led to an increase of the temperature of domain formation by about 8 °C (10 mol% SM at 18 °C (Fig. 4); 20 mol% at 26 °C and 30 mol% at 37 °C (Fig. 5), Table 1). Similar to the previous mixture (20 mol% SM), no domains with leaf-like structure were observed, but only the appearance of a large number of round  $L_o$  domains was detected at the temperature of their formation (Fig. 5d–f). If vesicles were left long enough (e.g. for about 30 min) at constant temperature to reach steady state, one or two large domains occupying in most cases 1/2 to 1/3 of their surface would form (data not shown).

#### 3.4. Control mixtures: PC/SPH/SM/CHOL 50/0/30/20 and 30/0/50/20

The purpose of these mixtures was to serve as controls for the PC/SPH/SM/CHOL 30/20/30/20 quaternary mixture, in which  $L_o/L_d$  phase separation was visualized when the total percentage of sphingolipids (SPH + SM) was 50 mol%. To establish the exact effect of SPH on the temperature of  $L_o$  domain formation, their fraction, domain number and fusion, two control mixtures were needed. In the first mixture the ratio SM/CHOL 30/20 was preserved. This control could give us an idea of the temperature of domain formation and the percentage of  $L_o$  fraction due only to this SM/CHOL 30/20 ratio, excluding the SPH influence. In the second PC/SPH/SM/CHOL 30/0/50/30 control mixture, 50 mol% SM mimicked the effect of total sphingolipid amount (SPH + SM). Thus, this control would

give us information on whether SPH exhibited phase behavior similar to that of SM in the raft mixtures. The  $L_o$  domains formed at comparatively lower temperatures, about 24 °C (Table 1), in the first control mixture PC/SPH/SM/CHOL 50/0/30/20 (Fig. 6a and b) compared with the EPC/SPH/ESM/CHOL 30/20/30/20 quaternary mixture, where they formed at 37 °C (Fig. 5d). Besides, the fraction of the dark  $L_o$  phase was smaller (Fig. 6c) than in EPC/SPH/ESM/CHOL 30/20/30/20 which is quite evident at 13 °C (Fig. 5f). No domains of irregular shape were observed.

In the second control mixture (PC/SPH/SM/CHOL 30/0/50/20), the formation of  $L_o$  domains occurred at 37 °C (Fig. 6d) just like in PC/SPH/ESM/CHOL 30/20/30/20 (Fig. 5d). However, the size of the domains in the control was significantly larger at 30 °C (Fig. 6e) and reached up to 1/2 of the vesicle surface at 13 °C (Fig. 6f), compared with PC/SPH/SM/CHOL 30/20/30/20 (Fig. 5e and f). Thus, the control mixtures demonstrate that SPH presence leads to stabilization (even amplification) of the formation of  $L_o$  phase by increasing the temperature of domain formation and their size. SPH exhibited properties similar to SM, but only in the presence of SM. The combined effect of both molecules, however, was less potent to form  $L_o$  domains compared to the net effect of SM. An effect of fragmentation of  $L_o$  phase was observed in the presence of SPH, which is visible in Fig. 5e and f compared to Fig. 6e and f. The distribution of domain sizes depends on the balance between the line tension, which tends to increase the size in order to reduce the total boundary length and entropy, and the electrostatic repulsions, which oppose  $L_o$  domain fusion [37–39]. SPH is a positively charged lipid molecule and it is expected to provide a greater contribution to the electrostatic repulsions over the line tension compared to non-containing SPH raft mixtures.

## 4. Discussion

Various studies suggest that the cellular functions of SPH are exerted more through its influence on the lipid phase behavior than its direct interaction with proteins [19,40,41]. The aim of our study was to examine the effect of SPH on domain morphology and its interactions with the raft-forming lipids, CHOL and SM.

Due to its relatively high melting point compared to the saturated glycerophospholipids (GPLs), SPH, like the other sphingolipids (SM and CER), was partially immiscible in the

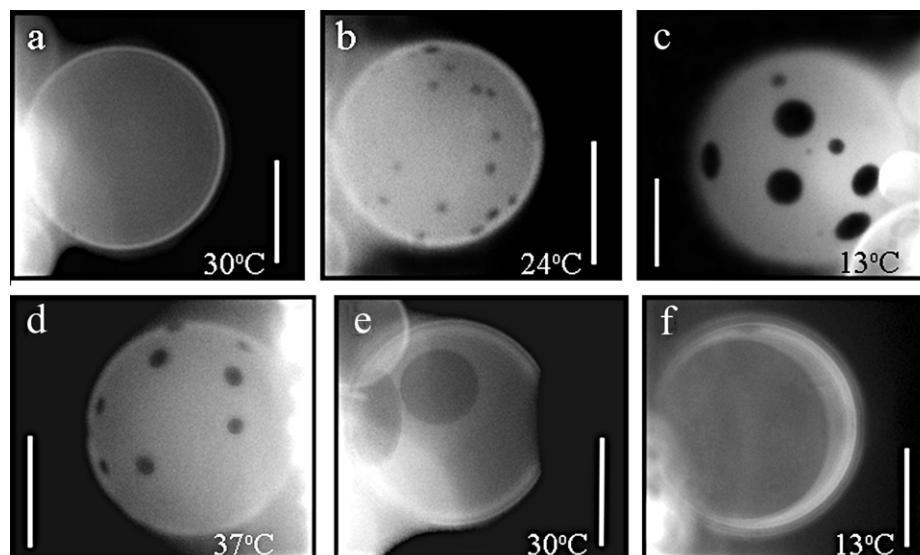


**Fig. 6.**  $L_0/L_d$  phase separation in a PC/SPH/SM/CHOL 50/0/30/20 control mixture (a–c). Homogenous vesicles from 30 to 25 °C (a). Formation of  $L_0$  domains at 24 °C (b). Domains increased their number and size with temperature decrease (c).  $L_0/L_d$  phase separation in a PC/SPH/SM/CHOL 30/0/50/20 control mixture (d–f). Formation of  $L_0$  domains at physiological temperature (d). Domains grew in size by fusion with temperature reduction (e and f). Bar 20  $\mu\text{m}$ .

glycerophospholipid matrix (Fig. 1b) [33,42,43]. It is known that SPH on one hand increases the phase transition temperature of GPLs which results in membrane fluidity decrease. On the other hand, SPH broadens the lipid phase transitions indicating low cooperativity and enlargement of the temperature range where domains in different phase states can coexist [13,44]. Despite the structural differences in the polar head group (phosphocholine in SM and a single hydroxyl group in CER and SPH), these sphingolipids form leaf-like gel domains (Fig. 1). Such kind of lipid segregation in membranes is possibly imposed by the hydrophobic mismatch between glycerophospholipids and sphingolipids. Leaf-like structure of sphingolipid domains is maintained by the strong van der Waals interactions between the saturated hydrocarbon chains and the electrostatic repulsion between the lipid dipoles (or between the net positive charges of SPH molecules) [32,45]. Because SPH differs in structure from SM and CER (a small polar head, a single OH group, only one hydrocarbon chain and the presence of a net positive charge), it is surprising that this molecule can form stable leaf-like domains like the other two-chain saturated lipids. Obviously the high degree of hydrophobicity, based on the saturation of the fatty acid chains, is a unifying factor which determines the lipid phase behavior of the gel/liquid state.

The addition of CHOL to the binary PC/SPH 80/20 mixture resulted in melting of SPH gel domains but only at ratios SPH/CHOL less than 1. Each 10 mol% CHOL decreased the temperature of domain formation by about 4 °C (Table 1). Such influence, but to a much larger extent, CHOL exerted on CER gel domains reducing the temperature of their formation by about 8 °C [46,47]. CHOL effect on the melting temperature of both sphingolipids (CER and SPH) is radically different from its effect on SM gel domains. The progressive enrichment of a PC/SM binary mixture with CHOL turned the gel/liquid phase coexistence into two immiscible liquid phases,  $L_0$  and  $L_d$  [30]. The high affinity of CHOL for phosphocholine-containing species, such as SM and saturated PC, and their specific interactions is a key factor for the formation of  $L_0$  phase [30]. However, the mechanism of CHOL effect on the structurally-identical hydrophobic parts of CER, SPH and SM is different and the possible reason is apparently the lack of a phosphocholine polar head group in SPH and CER molecules. CHOL and SPH in glycerophospholipid matrix did not form  $L_0$  phase, as shown in Figs. 2 and 3, neither did CHOL and CER [47]. The formation of  $L_0$  phase

and its visualization on the micron scale is a feature of the direct SM-CHOL interactions. The possible mechanism of melting of the other two sphingolipids, SPH and CER, by CHOL seems rather indirect. The presence of CHOL resulted in an increase of the molecular order parameter of the  $L_d$  phase, which in turn increased the miscibility of these two sphingolipids for this phase [46]. Thus, the fraction of gel domains gradually decreased with the increase of CHOL content (Fig. 3). Garmy et al. [15], using a Langmuir balance, reported a specific interaction between SPH and CHOL, leading to the formation of condensed lipid complexes. They suggested that SPH had a similar behavior in terms of SM interaction with CHOL. However, the visualization of the domain pattern in PC/SPH/CHOL (Figs. 2 and 3) and PC/SM/CHOL (Fig. 6) ternary mixtures showed radically different phase morphology of SPH and SM in the presence of CHOL.

Further complication of the model system by the addition of SM to the ternary PC/SPH/CHOL mixture demonstrated the competition between SPH and SM for the interaction with CHOL. Two types of phase morphology were distinguished in this series of experiments: dark domains with irregular shape at 20/10/20 SPH/SM/CHOL ratio and perfectly round  $L_0$  domains when the SM content was greater than or equal to that of SPH. In the first case, the presence of 10 mol% SM resulted in an increase of the temperature of gel domain formation by 8 °C (18 °C in the PC/SPH/SM/CHOL 50/20/10/20 mixture compared with the PC/SPH/CHOL 60/20/20 ternary mixture (10 °C) (Table 1)). Obviously the presence of SM leads to a decrease of the SPH miscibility in the ternary mixture. One possible mechanism is that SM and SPH form a gel phase with a higher melting temperature. Our results are consistent with the observation of Contreras et al. [19] which showed that SPH stabilizes the formation of gel domains in SM/CHOL membranes, by increasing the melting temperature and the cooperativity of the phase transition. It is noteworthy that SPH rigidifies the membranes, with or without CHOL, but the effect on the phase transition cooperativity is different. The broadening effect of CHOL on the phase transition is compensated by the presence of SPH unlike its effect on glycerophospholipid matrix. Below 10 °C the border of some  $L_0$  domains was clearly perturbed, other than circular (Fig. 4e–g). Despite the apparent lower value of the line tension of these domains, the specific properties of the liquid phase were preserved, since the domains grew in size by fusion. In the second

case, when SM mol% > SPH, only  $L_o/L_d$  phase separation was observed as the temperature of  $L_o$  domain formation raised progressively with increasing of the SM content in the mixture.  $L_o$  domains were visualized at physiological temperature in the PC/SPH/SM/CHOL 30/20/30/20 quaternary mixture (Fig. 5). The fraction of the dark  $L_o$  domains (for example, at 13 °C) was smaller compared to the PC/SPH/SM/CHOL 30/0/50/20 control mixture (Fig. 6d–f) and higher than that in PC/SPH/SM/CHOL 50/0/30/20 (Fig. 6a–c). Thus, we can conclude that SPH presence leads to enhanced fraction of domains in  $L_o$  phase and exhibits properties similar to those of SM, but only in the presence of SM. As shown above, SPH did not form typical  $L_o$  domains in the PC/SPH/CHOL ternary mixtures. The combined effect of SPH and SM as sphingolipids, however, was less pronounced compared to the net effect of SM on the formation of  $L_o$  phase.

In our previous studies, we showed that up to 10 mol% CER in PC/CER/SM/CHOL quaternary mixtures (50/10/20/20) did not interfere with the formation of  $L_o$  domains, i.e. the properties of a liquid phase were dominant [47]. For larger CER proportions (20, 30 mol%), however, gel domains formed at higher temperatures compared with the PC/CER/CHOL 80/10/20 and PC/CER 90/10 control mixtures, and the formation of  $L_o$  domains was shifted to lower temperatures compared with a raft-forming PC/SM/CHOL 60/20/20 mixture. We demonstrated that CER competed with CHOL for SM and formed more stable SM/CER gel domains leaving less available SM for the formation of  $L_o$  phase. The idea of the competition between CHOL and CER was not a new one and was proposed for the first time by Megha and London [48]. Later, using atomic force microscopy, other authors reported that the addition of CER to raft mixtures led to the formation of a third phase, thicker than the other two phases ( $L_o$  and  $L_d$ ) [49,50]. The formation of a third phase, obviously enriched in CER, within the  $L_o$  domains, is energetically beneficial, as the hydrophobic mismatch between the different phases is minimized.

The effect of SPH on the fluid properties of  $L_o$  domains was similar to that of CER (10 mol%), but at twice as large concentrations (20 mol%). We found that SPH stabilized the formation of the dark  $L_o$  fraction, but the question whether it participated in the form of a gel within the  $L_o$  domains or as a homogeneous component of this phase, similar to SM, remained unsolved. The competition between SPH and CHOL for interaction with SM occurred in proportions in which SM < SPH (Fig. 4). The properties of the  $L_o$  phase were preponderant when SM  $\geq$  SPH (Fig. 5) unlike CER effect (PC/CER/SM/CHOL 40/20/20/20) where the temperatures of gel domain formation and  $L_o$  were well distinguished [47]. Alanko et al. [51] showed that neither SPH nor sphinganine were able to displace CHOL from SM/CHOL domains, but the proportion SPH/SM/CHOL in their mixtures was 15/30/9, where the content of SM was more than twice that of SPH. This lipid ratio corresponds rather to SPH/SM/CHOL 20/20/20 and 20/30/20 in our experiments, where SM  $\geq$  SPH. In these cases, really, only  $L_o/L_d$  phase coexistence was observed and  $L_o$  domains formed at higher temperatures. Thus, in this line of arguments, it can be concluded that SPH exhibits a stabilizing effect on SM/CHOL domains.

## 6. Conclusions and biological implications

Interest in the sphingomyelin signaling pathway has increased very rapidly over the past few years. The first step of the SM pathway is the activation of cellular sphingomyelinases leading to the degradation of SM and the formation of ceramide. In our previous studies we reported that SM acts as an inhibitor of various forms of phospholipase  $A_2$  (PLA<sub>2</sub>) (secretory [52,53] and cytosolic [54]) and thus it plays a protective role in maintaining the integrity of cellular membranes, whereas the product of its degradation, ceramides,

are powerful activators of these enzymes [55]. It is supposed that the product of ceramide hydrolysis, sphingosine, also modulates the susceptibility of membrane phospholipids to PLA<sub>2</sub> [56–59]. However, it is noteworthy that while studies on sphingomyelin and ceramides and their role in cell biology are quite advanced, very little is currently clear about the biophysical properties of sphingosine and sphingosine-1-phosphate, known as second messengers in cell proliferation [7] and survival [60] and as functional participants in the “CER/S-1-P rheostat” [4].

Our research revealed that SPH exhibited a different domain pattern depending on the surrounding lipid matrix. In a glycerophospholipid matrix SPH segregated in gel leaf-like domains, whereas CHOL presence increased its miscibility by melting its gel domains in a concentration-dependent manner. We showed that SPH stabilized the formation of liquid-ordered phase, increasing the temperature of domain formation and thus their fraction. All these results implied that SPH is a modulator of the lipid phase behavior and thus it could exert its biological role, not only through direct binding to proteins, but also indirectly by influencing their sorting in membranes and thus modulating cell signaling. Very small amounts of SPH are needed to induce cellular response but the generation of SPH by enzyme reactions can reach high local concentrations in membranes.

Obviously, a study of the physico-chemical properties of all individual elements of the SM signaling pathway (SM, CER, SPH and SPH-1-P) is crucial for understanding their role in the modulation of various pathological processes in cells and for finding new ways of their control.

## Acknowledgments

Financial assistance was provided from Bulgarian Fund for Scientific Research (D002-69/2008, D002-212/2008, SMN60/2009, DTK 02/5-2009) and Operational Program “Human Resources Development” (BG 051PO001-3.3.04/42) co-financed by the European Social Fund of the European Union.

## References

- [1] E. Gulbins, S. Dreschers, B. Wilker, H. Grassme, J. Mol. Med. 82 (2004) 357–363.
- [2] T.A. Taha, T.D. Mullen, L.M. Obeid, Biochim. Biophys. Acta Rev. 1758 (2006) 2027–2036.
- [3] È. Takabe, S.W. Paugh, S. Milstien, S. Spiegel, Pharmacol. Rev. 60 (2008) 181–195.
- [4] O. Cuvillier, Biochim. Biophys. Acta 1585 (2002) 153–162.
- [5] C. Michel, G. van Echten-Deckert, J. Rother, K. Sandhoff, E. Wang, J. Biol. Chem. 272 (1997) 22432–22437.
- [6] M. Tani, M. Ito, Y. Igarashi, Cell Signal. 19 (2007) 229–237.
- [7] A. Olivera, S. Spiegel, Nature 365 (1993) 557–560.
- [8] N. Auge, M. Nikolova-Karakashian, S. Carpentier, S. Parthasarathy, A. Negre-Salvayre, R. Salvayre, A.H. Jr, Merril, T. Levade, J. Biol. Chem. 274 (1999) 21533–21538.
- [9] J.A. Hengst, J.M. Guilford, T.E. Fox, X. Wang, E.J. Conroy, J.K. Yun, Arch. Biochem. Biophys. 492 (2009) 62–73.
- [10] F. Lopez-Garcia, J. Villalain, J.C. Gomez-Fernandez, P.J. Quinn, Biophys. J. 66 (1994) 1991–2004.
- [11] H. Sasaki, H. Arai, M.J. Cocco, S.H. White, Biophys. J. 96 (2009) 2727–2733.
- [12] J.C. Gomez-Fernandez, J. Villalain, Chem. Phys. Lipids 96 (1998) 41–52.
- [13] A. Koiv, P. Mustonen, P.K. Kinnunen, Chem. Phys. Lipids 66 (1993) 123–134.
- [14] F. Lopez-Garcia, J. Villalain, J.C. Gomez-Fernandez, Biochim. Biophys. Acta 1236 (1995) 279–288.
- [15] N. Garmy, N. Taïeb, N. Yahi, J. Fantini, J. Lipid Res. 46 (2005) 36–45.
- [16] È. Ariga, W.D. Jarvis, R.K. Yu, J. Lipid Res. 39 (1998) 1–16.
- [17] E. Lloyd-Evans, A.J. Morgan, X. He, D.A. Smith, E. Elliot-Smith, D.J. Sillence, G.C. Churchill, E.H. Schuchman, A. Galione, F.M. Platt, Nat. Med. 14 (2008) 1247–1255.
- [18] J. Schroeder, H. Crane, J. Xia, D. Liotta, A.Jr. Merrill, J. Biol. Chem. 269 (1994) 3475–3481.
- [19] F.-X. Contreras, J. Sot, A. Alonso, F.M. Goni, Biophys. J. 90 (2006) 4085–4092.
- [20] Y.A. Hannun, R.M. Bell, Clin. Chim. Acta 185 (1989) 333–345.
- [21] F. Sakane, K. Yamada, H. Kanoh, FEBS Lett. 255 (1989) 409–413.
- [22] A. Matecki, T. Pawelczyk, Biochim. Biophys. Acta 1325 (1997) 287–296.
- [23] M. Angelova, D. Dimitrov, Faraday Discuss. Chem. Soc. 81 (1986) 303–311.
- [24] A.G. Ayuyan, F.S. Cohen, Biophys. J. 91 (2006) 2172–2183.

- [25] Y. Zhou, C.K. Berry, P.A. Storer, R.M. Raphael, *Biomaterials* 28 (2007) 1298–1306.
- [26] J. Zhao, J. Wu, H. Shao, F. Kong, N. Jain, G. Hunt, G. Feigenson, *Biochim. Biophys. Acta* 1768 (2007) 2777–2786.
- [27] L.A. Bagatolli, E. Gratton, *Biophys. J.* 79 (2000) 434–447.
- [28] L.A. Bagatolli, E. Gratton, *J. Fluorescence* 11 (2001) 141–160.
- [29] T. Baumgart, S.T. Hess, W.W. Webb, *Nature* 425 (2003) 821–824.
- [30] S.L. Veatch, S.L. Keller, *Biophys. J.* 85 (2003) 3074–3083.
- [31] K.Y.C. Lee, H.M. McConnell, *J. Phys. Chem.* 97 (1993) 9532–9539.
- [32] H.M. McConnell, *J. Phys. Chem.* 94 (1990) 4728–4731.
- [33] F. Lopez-Garcia, V. Micol, J. Villalain, J.C. Gomez-Fernandez, *Biochim. Biophys. Acta* 1153 (1993) 1–8.
- [34] C. Dietrich, L.A. Bagatolli, Z.N. Volovyk, N.L. Tompson, M. Levi, K. Jacobson, E. Gratton, *Biophys. J.* 80 (2001) 1417–1428.
- [35] S.A. Akimov, P.I. Kuzmin, J. Zimmerberg, *Rev. E Stat. Nonlin. Soft Matter Phys.* 75 (2007) 011919.
- [36] H. Rinia, M. Snel, J. van der Eerden, B. de Kruijff, *FEBS Lett.* 501 (2001) 92–96.
- [37] P.I. Kuzmin, S.A. Akimov, Y.A. Chizmadzhev, J. Zimmerberg, F.S. Cohen, *Biophys. J.* 88 (2005) 1120–1133.
- [38] S.L. Veatch, S.L. Keller, *Biochim. Biophys. Acta* 1746 (2005) 172–185.
- [39] C.D. Blanchette, W.C. Lin, T.V. Ratto, M.L. Longo, *Biophys. J.* 90 (2006) 4466–4478.
- [40] P. Mustonen, J. Lehtonen, A. Coiv, P.K. Kinnunen, *Biochemistry* 32 (1993) 5373–5380.
- [41] L.J. Siskind, S. Fluss, M.P. Bui, M. Colombini, *Biophys. J.* 88 (2005) 193A.
- [42] P.R. Maulik, G.G. Shipley, *Biophys. J.* 69 (1995) 1909–1916.
- [43] J. Shah, R.I. Atienza, A.V. Duclos, A.V. Rawlings, Z. Dong, G.G. Shipley, *J. Lipid Res.* 36 (1995) 1936–1944.
- [44] V.M.J. Saily, J.M. Alakoskela, S.J. Ryhanen, M. Karttunen, P.K.J. Kinnunen, *Langmuir* 19 (2003) 8956–8963.
- [45] S. Hartel, M.L. Fanani, B. Maggio, *Biophys. J.* 88 (2005) 287–304.
- [46] G. Staneva, C. Chachaty, C. Wolf, K. Koumanov, P.J. Quinn, *Biochim. Biophys. Acta* 1778 (2008) 2727–2739.
- [47] G. Staneva, A. Momchilova, C. Wolf, P.J. Quinn, K. Koumanov, *Biochim. Biophys. Acta* 1788 (2009) 666–675.
- [48] Megha, E. London, *J. Biol. Chem.* 279 (2003) 9997–10,004.
- [49] S. Chiantia, N. Kahya, J. Ries, P. Schwille, *Biophys. J.* 90 (2006) 4500–4508.
- [50] I. Johnston, L. Johnston, *Biochim. Biophys. Acta* 1778 (2008) 185–197.
- [51] S.M.K. Alanko, K.K. Halling, S. Maunula, J.P. Slotte, B. Ramstedt, *Biochim. Biophys. Acta* 1715 (2005) 111–121.
- [52] K. Koumanov, C. Wolf, G. Bereziat, *Biochem. J.* 326 (1997) 227–233.
- [53] K.S. Koumanov, P.J. Quinn, G. Bereziat, C. Wolf, *Biochem. J.* 336 (1998) 625–630.
- [54] E. Klapisz, J. Masliah, G. Bereziat, C. Wolf, K.S. Koumanov, *J. Lipid Res.* 41 (2000) 1680–1688.
- [55] K.S. Koumanov, A.B. Momchilova, P.J. Quinn, C. Wolf, *Biochem. J.* 363 (2002) 45–51.
- [56] R.C. Franson, L.K. Harris, S.S. Ghosh, M.D. Rosenthal, *Biochim. Biophys. Acta* 1136 (1992) 169–174.
- [57] T. Neitcheva, D. Peeva, *Int. J. Biochem. Cell Biol.* 27 (1995) 995–1001.
- [58] J.W. Huang, E.M. Goldberg, R. Zidovetzki, *Biochem. Biophys. Res. Commun.* 220 (1996) 834–838.
- [59] H. Nakamura, T. Hirabayashi, A. Someya, M. Shimizu, T. Murayama, *Eur. J. Pharmacol.* 484 (2004) 9–17.
- [60] G.P. Cuvillier, B. Kleuser, P.G. Vanek, O.A. Coso, J.S. Gutkind, S. Spiegel, *Nature* 381 (1996) 800–803.